NACA

RESEARCH MEMORANDUM

WIND-TUNNEL INVESTIGATION AT TRANSONIC SPEEDS OF A

JET CONTROL ON AN 80° DELTA-WING MISSILE

By Thomas R. Turner and Raymond D. Vogler

Langley Aeronautical Laboratory
Langley Field, Va.

NATIONAL ADVISORY COMMITTEE
FOR AERONAUTICS

WASHINGTON

November 1, 1955

NACA RM L55H22

NATIONAL ADVISORY COMMITTEE FOR AERONAUTICS

RESEARCH MEMORANDUM

WIND-TUNNEL INVESTIGATION AT TRANSONIC SPEEDS OF A

JET CONTROL ON AN 80° DELTA-WING MISSILE

By Thomas R. Turner and Raymond D. Vogler

SUMMARY

An investigation was made in the Langley high-speed 7- by 10-foot tunnel at Mach numbers from 0.60 to 1.15 of three missile models with cruciform delta wings swept back 80° and equipped with jet controls to determine the effectiveness of the controls when using ram or mechanically compressed air for operation. For comparison, data were also obtained using a spoiler of equal span.

The results indicated that the jet control is effective throughout the angle-of-attack and Mach number range investigated. The magnitude of the effectiveness increases with increase in the momentum of the jet. For jet configurations using ram air, exit-to-inlet area ratios as high as 1.28 were increasingly effective.

INTRODUCTION

There has been considerable interest recently in the use of air jets as a means of simplifying the control of missiles and airplanes. The results of references 1 to 4 have shown that if either stream ram air or compressed air is exhausted normal to a wing surface it will change the lift over the wing in a manner similar to that produced by a spoiler or split flap and thus provide a means of controlling the aircraft's attitude.

The present paper presents the results of an investigation at transonic speeds of a jet control on three missile configurations having delta cruciform wings with the leading edge swept back 80°. Two of the models used air at stream ram pressure picked up by scoops attached to the wing tips. The third model was supplied with air at several atmospheres of pressure from a compressed-air system.

For comparative purposes, two of the models were also tested with spoilers located at the wing trailing edge.

SYMBOLS AND COEFFICIENTS

The forces and moments measured on the model are presented about an orthogonal system of axes. The longitudinal axis is parallel to the free air stream and the lateral axis is in the horizontal wing chord plane. The origin of the axes is on the fuselage center line at a longitudinal position as indicated on the drawing of each model (figs. 1, 2, and 3).

C_L lift coefficient, $\dfrac{\text{Lift}}{qS_1}$

C_D drag coefficient, $\dfrac{\text{Drag}}{qS_3}$

C_m pitching-moment coefficient, $\dfrac{\text{Pitching moment}}{qS_1\bar{c}}$

C_l rolling-moment coefficient produced by the control,

$\qquad\qquad\dfrac{\text{Rolling moment}}{qS_2 b}$

S_1 total wing area of two panels, sq ft

S_2 total wing area of four panels, sq ft

S_3 exposed wing area of four panels, sq ft

q dynamic pressure, $\dfrac{\rho V^2}{2}$, lb/sq ft

ρ mass density of air, slugs/cu ft

V free-stream velocity, ft/sec

b wing span (wing tip to opposite wing tip), ft

$\bar{c}$ mean aerodynamic chord of wing, ft

C_μ momentum coefficient, $\dfrac{Q'V_j}{gqS}$

Q'   quantity of air used in control jets, lb/sec

S   total area of wing panels having controls attached, sq ft

V_j jet velocity associated with isentropic expansion to the crit-
            ical pressure ratio (0.528) at the jet exit, ft/sec

g   acceleration of gravity, ft/sec^2

C_{l_p} damping-in-roll coefficient, $\dfrac{\partial C_l}{\partial \dfrac{pb}{2V}}$

$\dfrac{pb}{2V}$ wing-tip helix angle, radians

p   rate of roll, radians/sec

$\dfrac{P}{H_o}$ ratio of static pressure in control manifold to free stream
            total head

M   Mach number

R   Reynolds number

α angle of attack, deg

MODELS AND APPARATUS

The geometric characteristics of the three models used in the inves-
tigation are given in figures 1, 2, and 3 and will be referred to as
models 1, 2, and 3, respectively. Model 1 was tested on the forced-roll
apparatus (ref. 5), model 2 was a sting-mounted model, and model 3, a
semispan model, was tested using the transonic bump.

Model 1 had cruciform wings made of aluminum alloy covered with
mahogany with the leading edge swept back 80°. The 5-inch-diameter fuse-
lage was made of laminated wood. The air at ram pressure for the jet
control was obtained from 0.8-inch inside diameter cylindrical air scoops
located near the wing tips (fig. 1). The air was ducted through the wing
to a series of 0.120-inch-diameter holes drilled into the manifold
0.187 inch ahead of the trailing edge. The larger span jet control con-
sisted of 28 holes extending from 0.26 to 0.82 semispan. The smaller
span jet control extended from 0.54 to 0.82 semispan and consisted of

14 holes. The larger span jet control was tested at two chordwise positions (models 1(A) and 1(C)), and for comparative purposes, a flap-type or wedge trailing-edge spoiler (model 1(B)) having the same span and location was investigated.

Model 2 was very similar to model 1 in basic plan form. The wing profile was different because the wing of model 2 was made of 3/8-inch aluminum plate. Part of the basic wing at the trailing edge was removed and replaced by a box manifold which extended beyond the wing tips. The forward side of the box beyond the wing tip served as the air inlet to the manifold. The 39 jet holes were inclined forward 20° and placed 0.187 inch ahead of the trailing edge. The jet hole diameters were 0.062, 0.090, 0.120, and 0.150 inch for the various configurations of model 2(A). For the spoiler configuration (model 2(B)) a box without holes and not extending beyond the wing tip of the basic wing was attached to the trailing edge, and spoilers projecting 0.5 inch above the surface of the box were attached to the trailing edge of the box.

The semispan reflection-plane model (fig. 3) had a wing made of 1/8-inch steel plate and a fuselage made of tubing except for the nose which was solid. The jet manifold was attached to the trailing edge of the wing and opened into the hollow fuselage. Compressed air introduced into the fuselage flowed through the manifold and out the holes at the trailing edge of the wing. Sets of jet holes of two diameters, 0.015 and 0.020 inch, located 0.045 inch ahead of the wing trailing edge were investigated.

The forces and moments of the sting-mounted models (figs. 1 and 2) were measured by an electrical strain-gage balance incorporated inside the model and were recorded by calibrated potentiometers. In obtaining the damping-in-roll data of model 1, the model was forced to roll about its longitudinal axis at various known rates.

The semispan model (fig. 3) was mounted on an electrical strain-gage balance enclosed within a transonic bump. Compressed air was introduced into the model through a flexible hose within the bump balance chamber. The amount of air used was measured with a flowmeter. The forces and moments were recorded with calibrated recording potentiometers.

TESTS

Forced-roll tests were made of model 1 at zero angle of attack through a Mach number range of 0.60 to 0.98 to determine the damping-in-roll coefficients and wing-tip helix angle. Data were obtained for jet controls of two different spans with 0.120-inch-diameter jet holes located 0.187 inch ahead of the trailing edge. A wedge spoiler was also tested.

Static tests of these same configurations were made at $\alpha = 0°$ · and $\alpha = \pm 4.2°$ to determine rolling-moment coefficients. In addition, forced-roll tests were made with the jet holes located 6.3 inches ahead of the trailing edge of the wing.

Static tests of model 2 were made through a Mach number range from 0.60 to 0.95 and angle-of-attack range from 0° to 23° with jet holes of various diameters (0.062 inch to 0.150 inch) located 0.187 inch ahead of the trailing edge and extending spanwise from the fuselage (0.26b/2) to the tip of the basic wing. A spoiler of 0.5-inch projection and having the same span as the jet control was attached to the trailing edge and tested for comparison with the jet control.

Model 3 was tested through an angle-of-attack range from -8° to 12° at Mach numbers of 0.90 and 1.15. Jet holes of two diameters (0.015 in. and 0.020 in.) were located 0.045 inch ahead of the trailing edge and extended spanwise from the surface of the fuselage (0.30b/2) to 0.95 semi-span. Air under various gage pressures up to 100 pounds per square inch was forced through the jet holes.

The variation of Reynolds number with Mach number for the three models is shown in figure 4.

CORRECTIONS

The blocking corrections which were applied to the dynamic pressure and Mach number for the sting-mounted models were determined by the method of reference 6. The difference in static pressure of the free stream and the pressure at the base of the model was measured, and the drag coefficients have been corrected by an increment based on this pressure difference and the base area of the model. This pressure difference was not the same for all configurations, but the correction in any case was only a small percentage of the total drag coefficient.

No corrections to the data of the reflection-plane model have been applied. The usual wind-tunnel blockage and jet-boundary corrections are considered negligible on account of the small size of the model in relation to the size of the tunnel test section.

RESULTS AND DISCUSSION

General Remarks

All rolling-moment data were obtained with the control operating on all four wing panels. The pitching-moment data are based on the controls operating only on the two horizontal panels. For some tests, indicated

on the figures, the roll control was operating on the vertical panels
while pitching-moment data were being obtained.

Model 1

The rolling characteristics of model 1 with air-jet controls of two
spans and a wedge spoiler of 0.33-inch projection are given in figure 5
with some unpublished data of the same model in rocket flight. The larger
span control operated with ram air produces a $\frac{pb}{2V}$ of approximately 0.056
which is about 10 percent less than that produced by a wedge spoiler of
approximately $0.01\bar{c}$ projection. There is little variation of $\frac{pb}{2V}$ with
Mach number below 0.90. The tunnel results agree well with the unpublished
results obtained in free flight on the same model. The controls had little
effect on the damping-in-roll coefficients. All data taken during forced
roll were at $\alpha = 0°$.

Static rolling-moment coefficients were obtained (fig. 6) at $\alpha = 0°$
and $\alpha = \pm 4.2°$ for the same configurations and Mach number range. At
$\alpha = 0°$, these rolling-moment coefficients agree very well with the values
obtained from the forced-roll tests (fig. 5) and this agreement is an
indication of the accuracy of the test technique. Lift coefficients
at $\alpha = 0°$ and $\pm 4.2°$ were also obtained for the plain wing and presented
in figure 7. The angle-of-attack range was limited by structural consid-
erations of the model.

In order to get an indication of the static pressure inside the
control manifold, three orifices were installed. One orifice was located
at midsemispan, one near the wing tip, and one near the fuselage. Fig-
ure 8 indicates that the ratio of pressure in the manifold to the free
stream total head is between 0.875 and 1.00. This pressure ratio decreases
with increase in Mach number and is greater for the shorter span control
than the longer.

The longer span jet control was moved forward 6.3 inches ahead of
the wing trailing edge, and at this position small rolling moments in the
reverse direction were indicated as shown in figure 9. These results
agree with the results of reference 7 in that location of jet controls
or spoilers ahead of the trailing edge reduced or reversed the
effectiveness.

Model 2

The basic plan form of model 2 (fig. 2) was the same as model 1.
The span of the jet spoiler was from 0.26 to 0.97 semispan and jet holes
of four diameters were investigated. The variation of static rolling-
moment coefficient with angle of attack, Mach number, and jet hole diameter

is shown in figure 10. Increased coefficients were obtained with increased hole diameter at all angles of attack and Mach numbers. Extrapolation of the curves would indicate that jet holes larger than the largest tested probably would give slightly larger rolling-moment coefficients with the size ram inlet used. The 0.150-inch-diameter holes had a total area 28 percent larger than the ram inlet area.

Some tests were made with jet holes on the bottom surface of the horizontal wing panels acting as a pitch control. This configuration gave considerable pitch control and had little effect on the static longitudinal stability of the plain-wing model (fig. 11). Operating the rolling jets on the vertical panels apparently did not affect the pitching characteristics of the jets on the horizontal panels. More complete characteristics in pitch of the plain-wing model and the model with the largest jet holes investigated are given in figure 12. The lift coefficients of the model with and without the jet controls producing roll on all four panels are given in figure 13. The jet controls have little effect on the total lift on the model.

For comparison with the jet control, a spoiler of 1/2-inch projection attached to the trailing edge of each wing panel was investigated. The jet control with holes 0.150 inch in diameter was from 40 to 60 percent as effective as the 1/2-inch spoiler (fig. 14). Both the spoiler and jet control lost some effectiveness at high angles of attack, and the spoiler lost as the Mach number increased, but the jet control lost effectiveness only above a Mach number of 0.90. The increment of drag coefficient of the jet control is considerably less than that of the spoiler at low angles of attack. (See figs. 12 and 15.) Drag comparison based on these data at high angles of attack would not be valid since the spoiler and jet control were on opposite sides of the horizontal wing.

Model 3

Force and moment data with jet controls on model 3 were obtained at M = 0.90 and 1.15 and are presented in figures 16 to 18. As in the sting-mounted models, rolling-moment and pitching-moment coefficients are based on controls operating on four panels and two panels, respectively. The maximum gage pressure used to obtain the largest momentum coefficients was about 75 psi with the 0.020-inch holes and about 100 psi with the 0.015-inch holes. The jet control rolling- and pitching-moment and lift coefficients varied almost directly with momentum coefficient. At a Mach number of 1.15, there was little difference between the two jet hole sizes for equal momentum coefficients; but, at a Mach number of 0.90, different size jet holes produced some differences in rolling-moment and lift coefficients at a constant momentum coefficient.

An estimate of the jet-thrust effect on the force and moment coefficients was made using the relation:

$$\text{Thrust} = \frac{Q'V_j}{g} + (\text{Jet area}) \times (\text{Static pressure difference between jet exit and free stream})$$

The jet thrust center was assumed to be at the center of the group of jet holes. After reducing the thrust to force and moment coefficients, the results represented by the dashed lines in figure 19 were obtained. The computed values resulting from jet thrust are 25 to 30 percent of the total values obtained.

CONCLUDING REMARKS

A wind-tunnel investigation was made at Mach numbers from 0.60 to 1.15 of three missile models with cruciform delta wings swept back 80° and equipped with air-jet controls to determine the effectiveness of the controls in producing rolling and pitching moments when using ram or mechanically compressed air for their operation.

The results indicated that the jet control produces effectiveness throughout the angle-of-attack and Mach number range investigated. The magnitude of the effectiveness increased with increase in the momentum of the jet. For jet configurations using ram air, exit-to-inlet area ratios as high as 1.28 were increasingly effective.

Langley Aeronautical Laboratory,
National Advisory Committee for Aeronautics,
Langley Field, Va., August 15, 1955.

REFERENCES

1. Ballentine, Donald C., and Barnard, George A..: Two-Dimensional Wind-Tunnel Tests of a Jet-Type Spoiler on an NACA 64A010 Airfoil Section Equipped With High-Lift Devices. Aero. Rep. 862, David W. Taylor Model Basin, Navy Dept., June 1954.

2. Lowry, John G., and Turner, Thomas R.: Low-Speed Wind-Tunnel Investigation of a Jet Control on a 35° Swept Wing. NACA RM L53I09a, 1953.

3. Göthert, B.: Effectiveness of a Spoiler at High Subsonic Speeds. Reps. and Translations No. 364, British M.O.S.(A) Völkenrode, Feb. 1947.

4. Attinello, John S.: An Air-Jet Spoiler. NAVAER Rep. DR-1579, Bur. Aero., Aug. 1953.

5. Kuhn, Richard E., and Wiggins, James W.: Wind-Tunnel Investigation To Determine the Aerodynamic Characteristics in Steady Roll of a Model at High Subsonic Speeds. NACA RM L52K24, 1953.

6. Hensel, Rudolph W.: Rectangular-Wind-Tunnel Blocking Corrections Using the Velocity-Ratio Method. NACA TN 2372, 1951.

7. Wiley, Harleth G.: A Wind-Tunnel Investigation at High Subsonic Speeds of the Lateral Control Characteristics of Various Plain Spoiler Configurations on a 3-Percent-Thick 60° Delta Wing. NACA RM L54D01, 1954.

model (A)

origin of axes (0.51c̄)

model (B)

Wing section at fuselage

model (C)

C̄ = 36.4
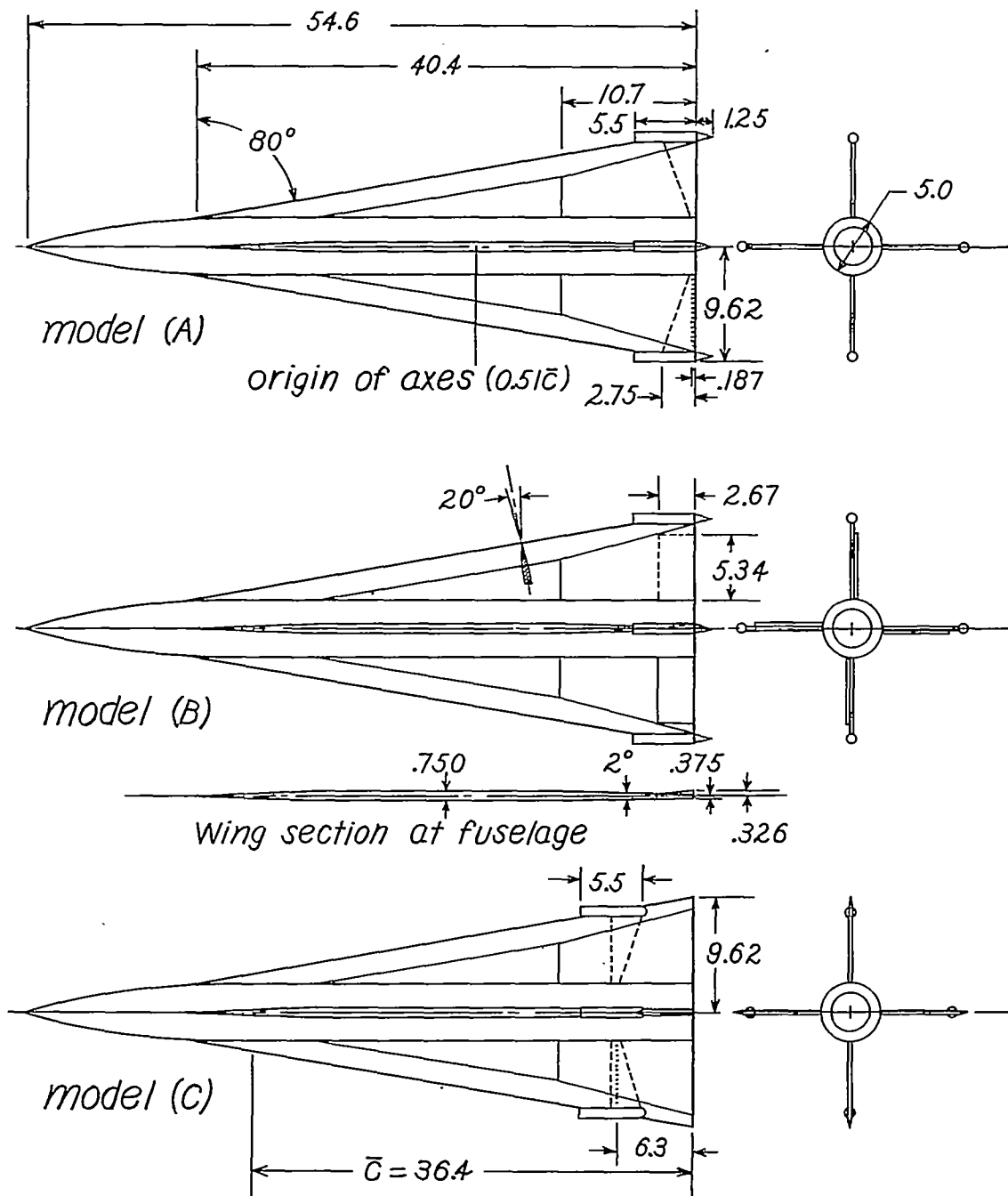
(a) General dimensions.

Figure 1.- Model 1 showing jet control (A and C) and wedge spoilers (B). Dimensions in inches.

model (A)

0.187

0.31

5.34

A   A

0.87

$\frac{1}{16} \times 45°$ chamfer

.035

2.75

section A-A

20°

$\frac{1}{16}$ 0.25

0.120 D on $\frac{3}{16}$ centers
28 holes

model (C)

0.31

5.34   A   A

2.75

6.3

section A-A

20°

$\frac{1}{16}$ 0.25
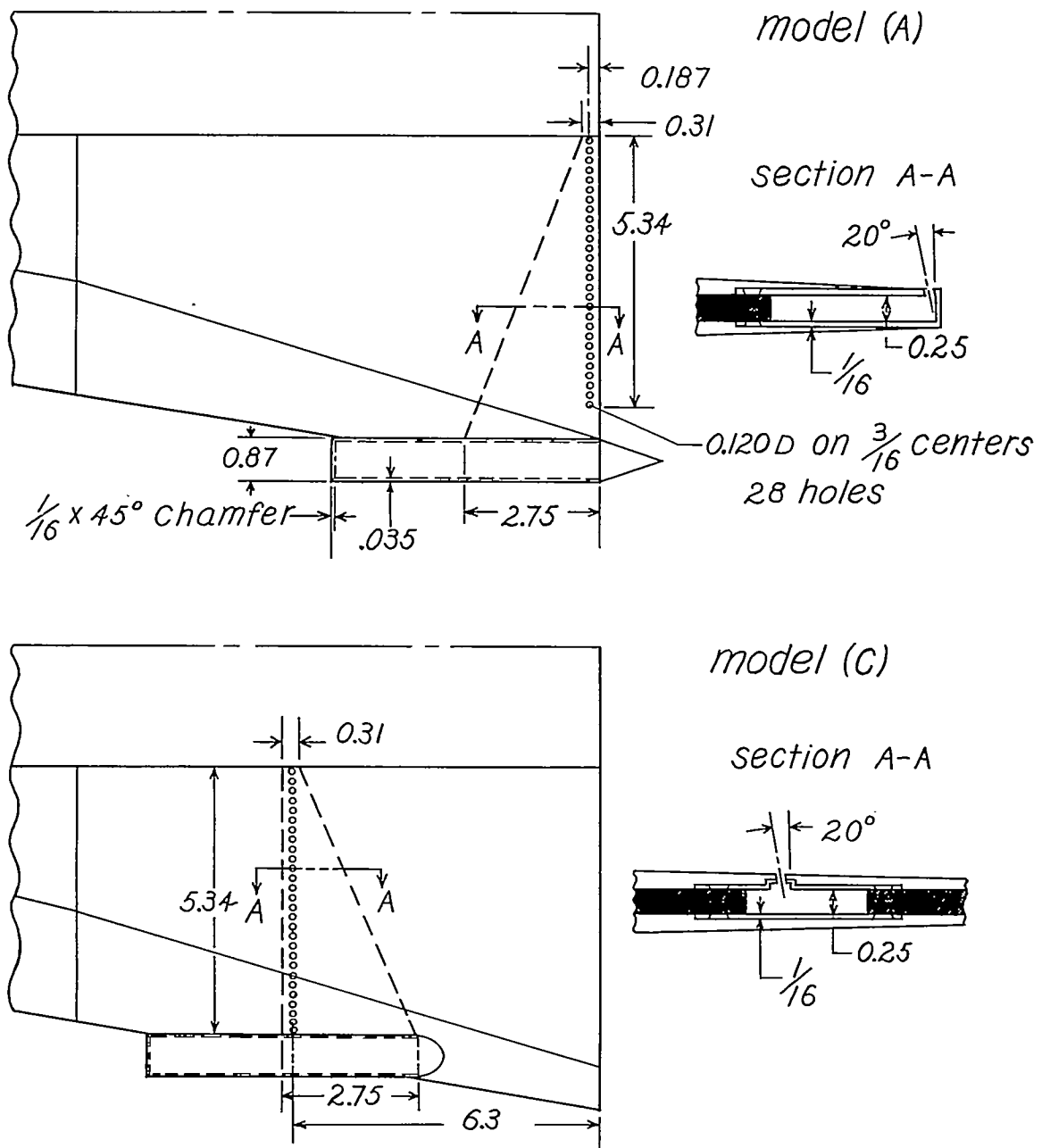
(b) Jet control details.

Figure 1.- Concluded.
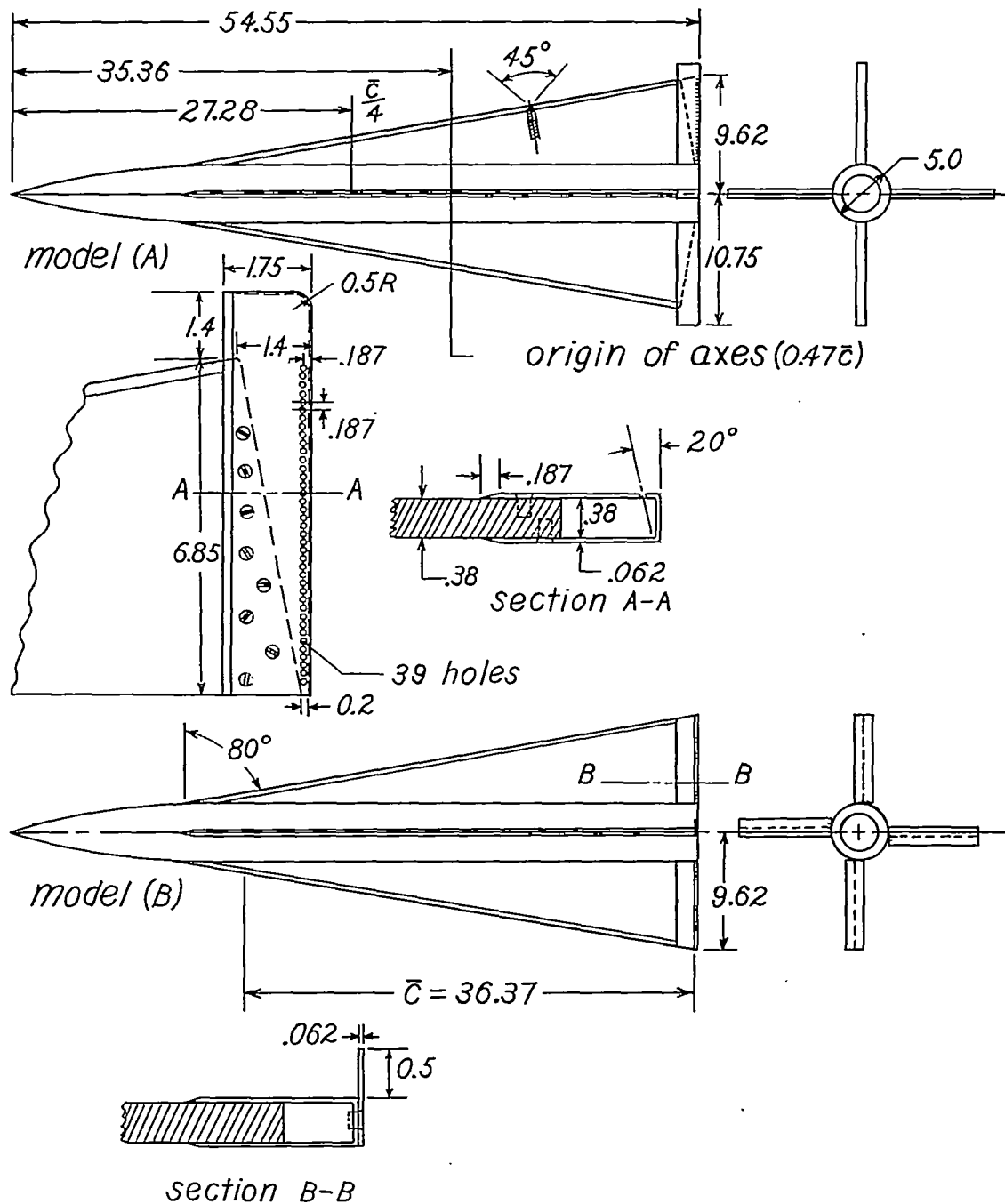
Figure 2.- Model 2 showing jet control (A) and spoilers (B). Dimensions in inches.

Section A-A

20°

.020

.025

0.125

.250

.015D and .020D holes
on .030 centers
origin of axes (0.60c̄)

A

A

C̄/4

80°

C̄ = 6.33

1.67

.062

0.5

10.0

0.50
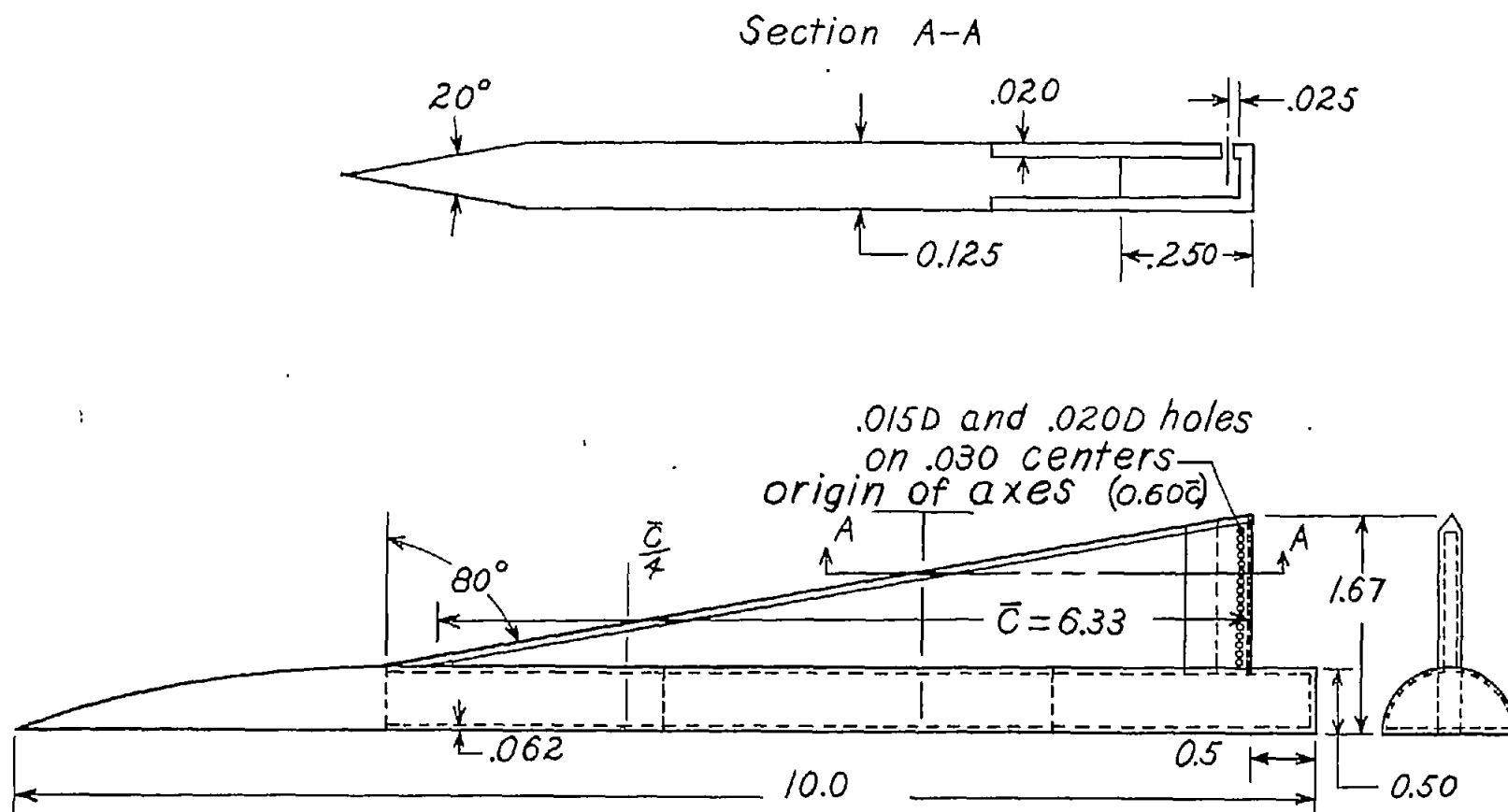
Figure 3.- Model 3 showing jet control operated with compressed air.
Dimensions in inches.
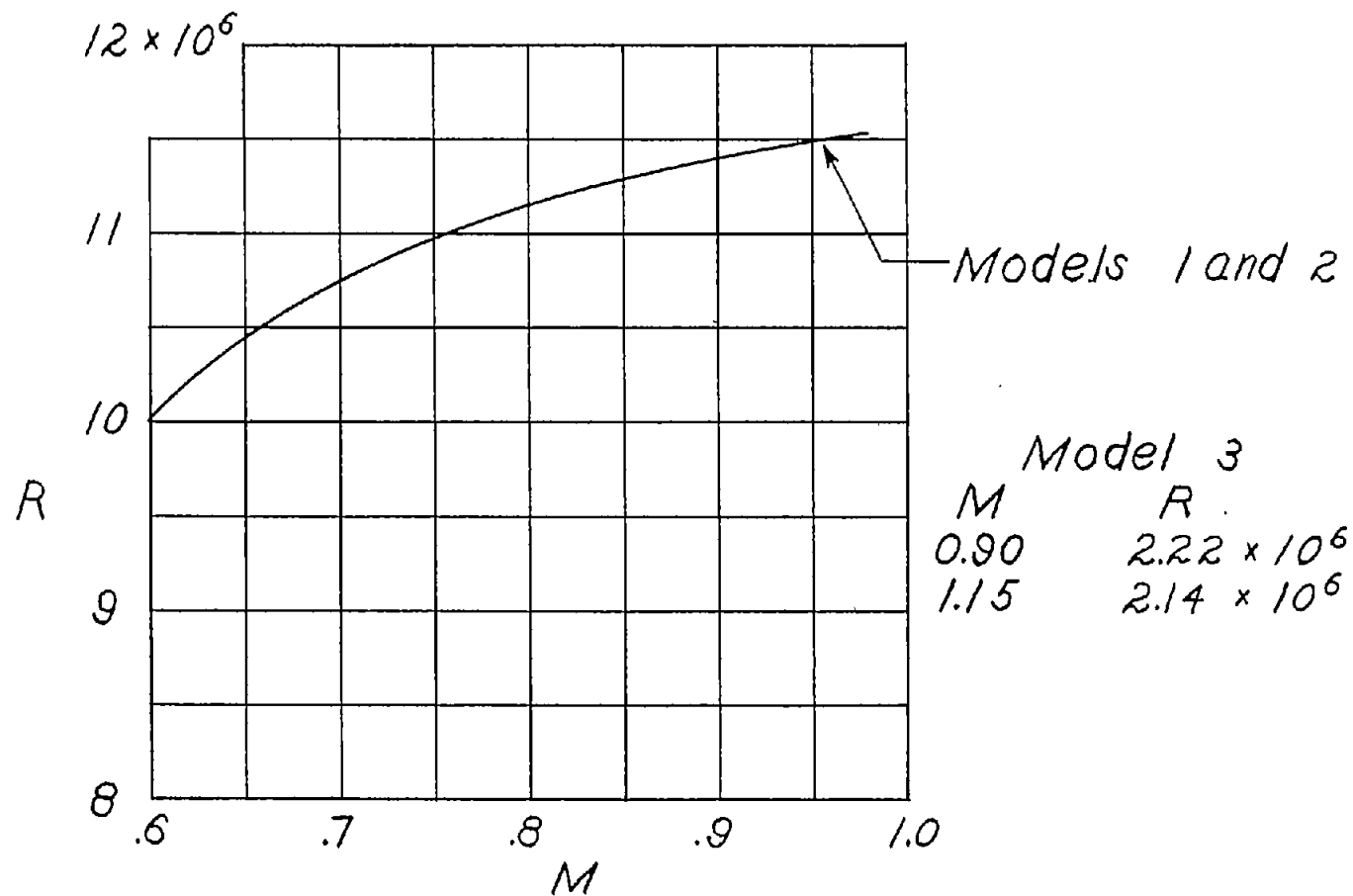
Figure 4.- Variation of mean Reynolds number with Mach number.

control	model	control location
spoiler	I(B)	0.26 $\frac{b}{2}$ to 0.82 $\frac{b}{2}$
jet	I(A)	$\}$ .54 $\frac{b}{2}$ to .82 $\frac{b}{2}$
	I(A) rocket	
	I(A)	$\}$ .26 $\frac{b}{2}$ to .82 $\frac{b}{2}$
	I(A) rocket	
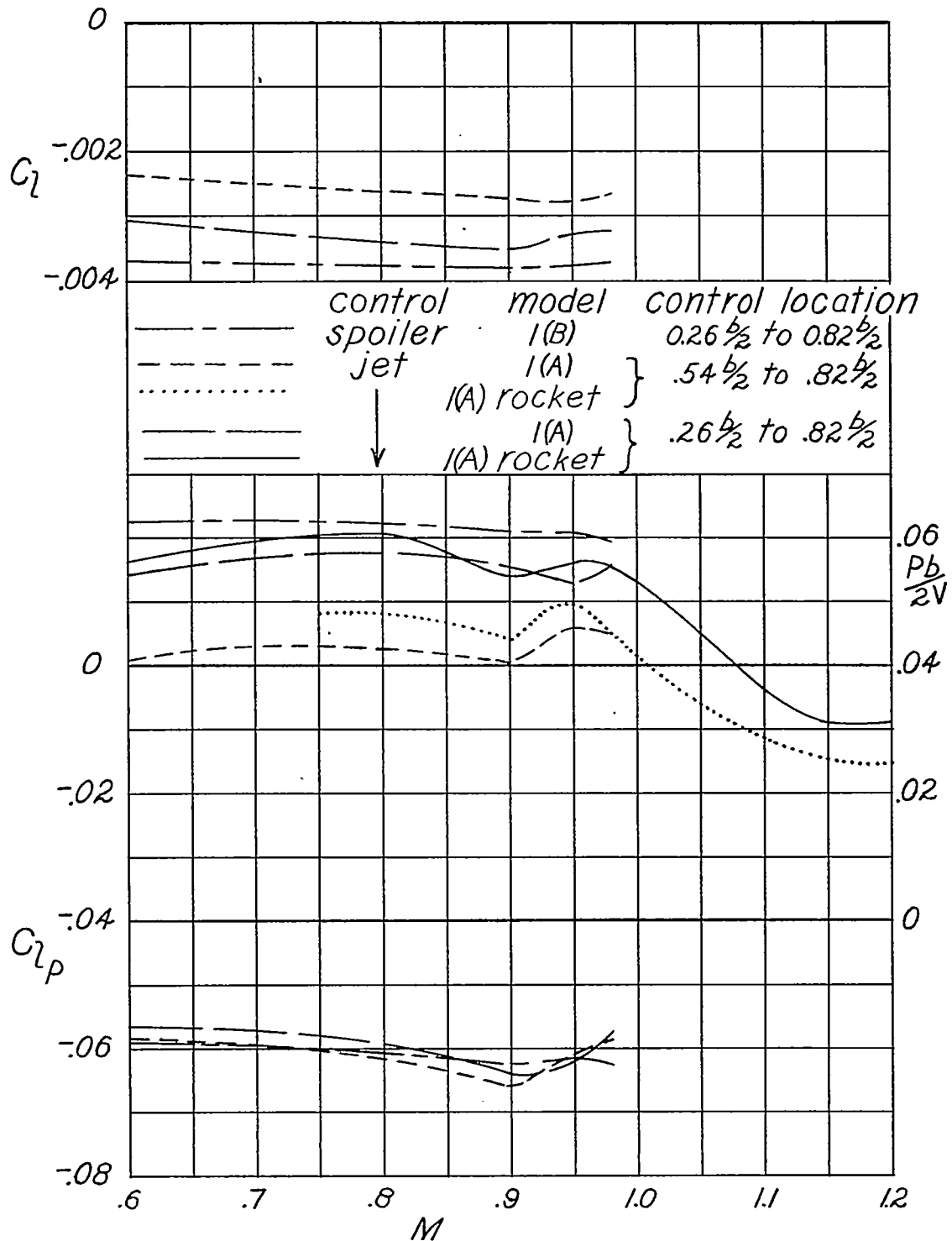
Figure 5.- Rolling characteristics of models with various control configu-
rations obtained with model under forced roll at α = 0° in wind tunnel
and in free flight.
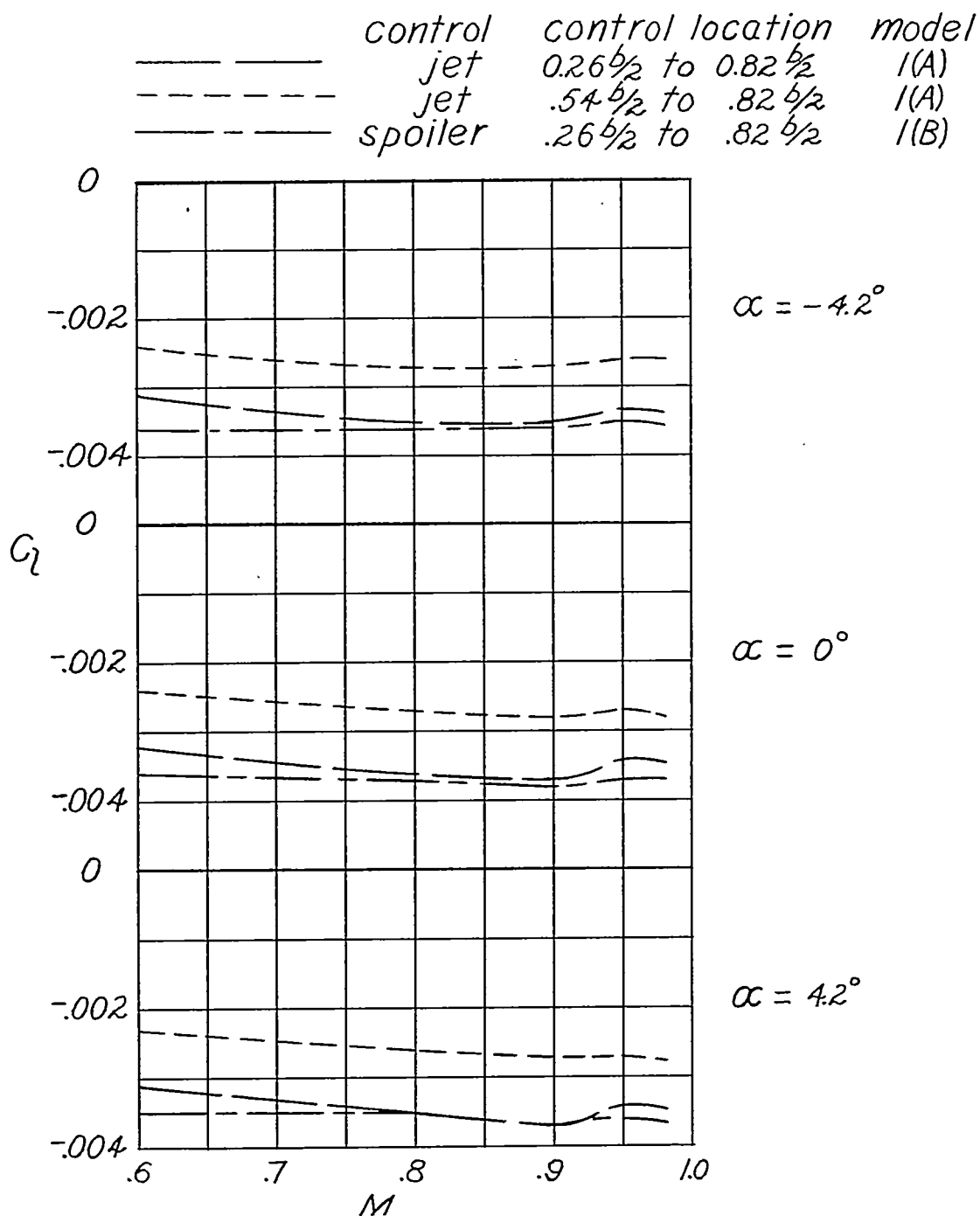
Figure 6.- Rolling-moment coefficient variation with Mach number of model 1 (A and B) with various control configurations obtained under model static conditions.
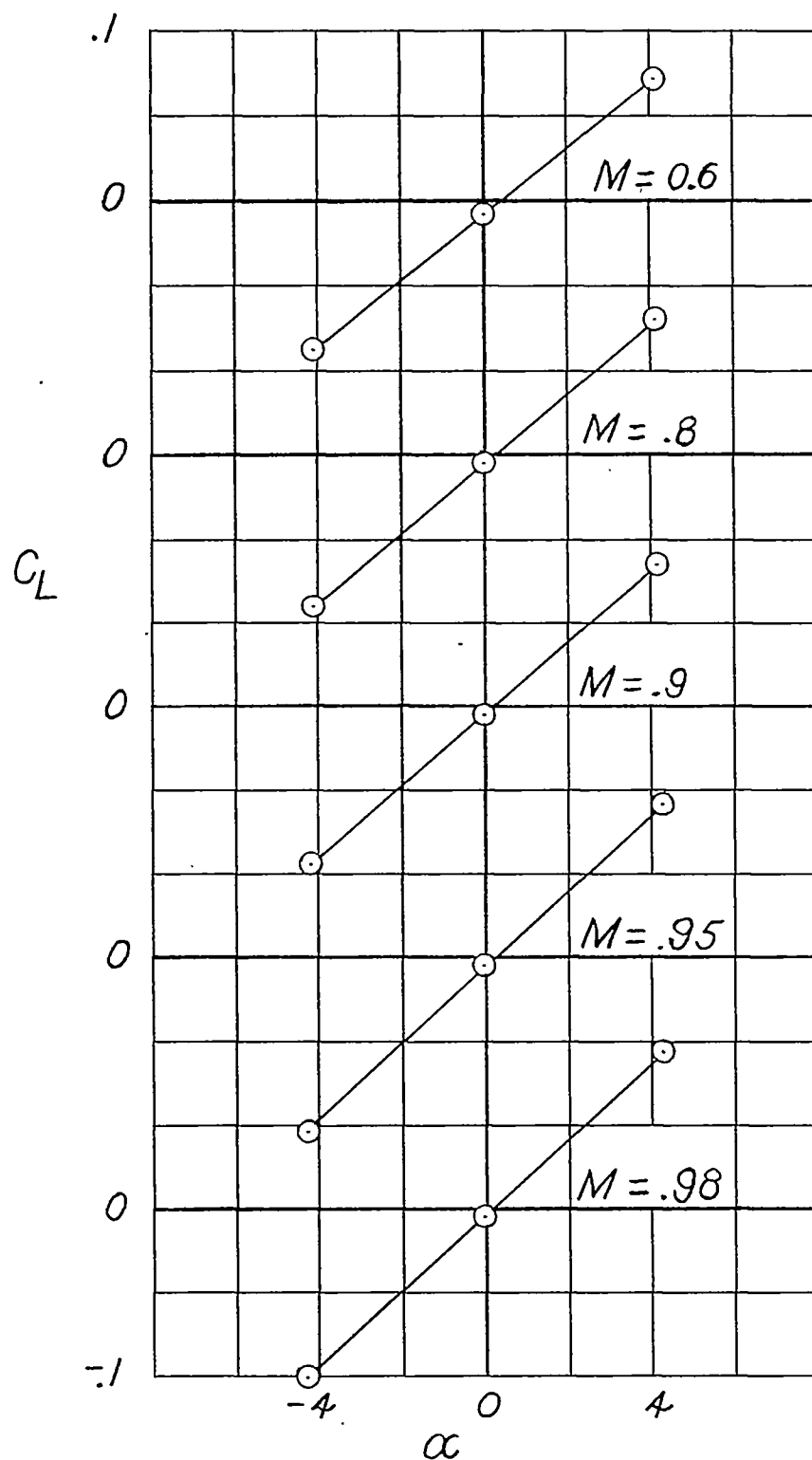
Figure 7.- Variation of lift coefficient with angle of attack of the plain-wing (jet holes sealed) model 1(A).

NACA RM L55H22
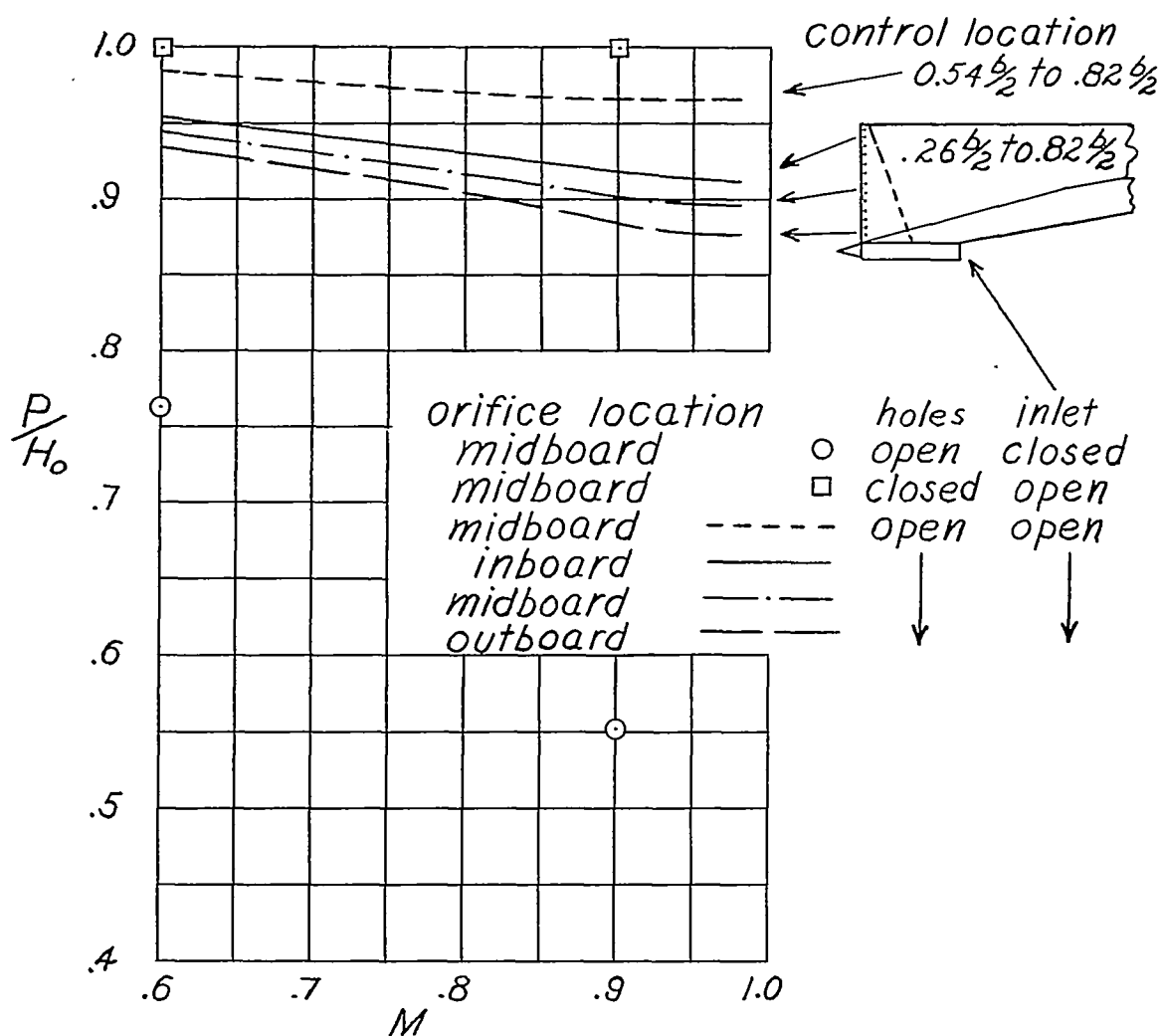
Figure 8.- Pressure ratios inside the jet control manifold of model 1(A) under static conditions.
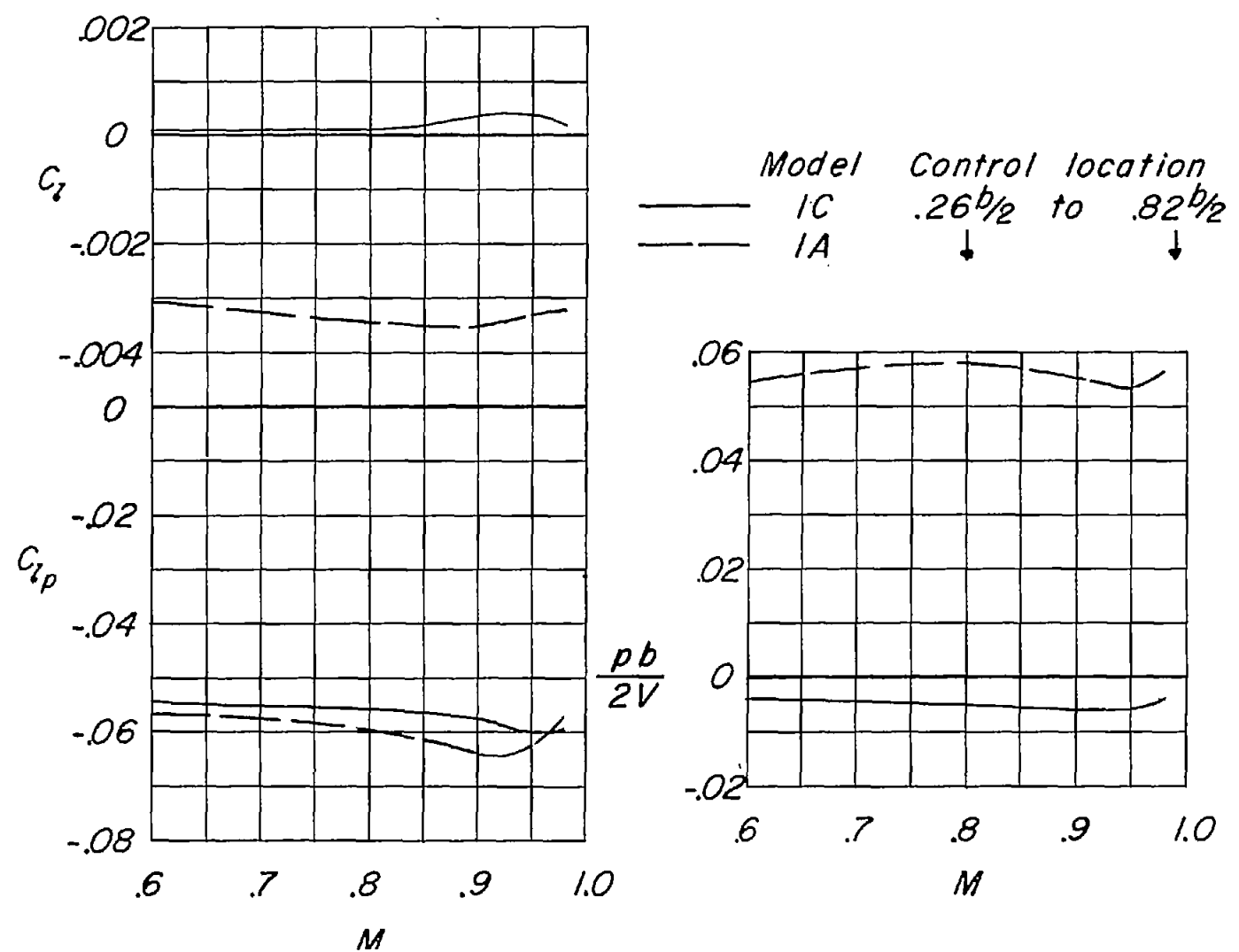
Figure 9.- Effect of moving jet holes from trailing edge (model 1(A)) to a position 6.3 inches ahead of trailing edge (model 1(C)). $\alpha = 0^\circ$.
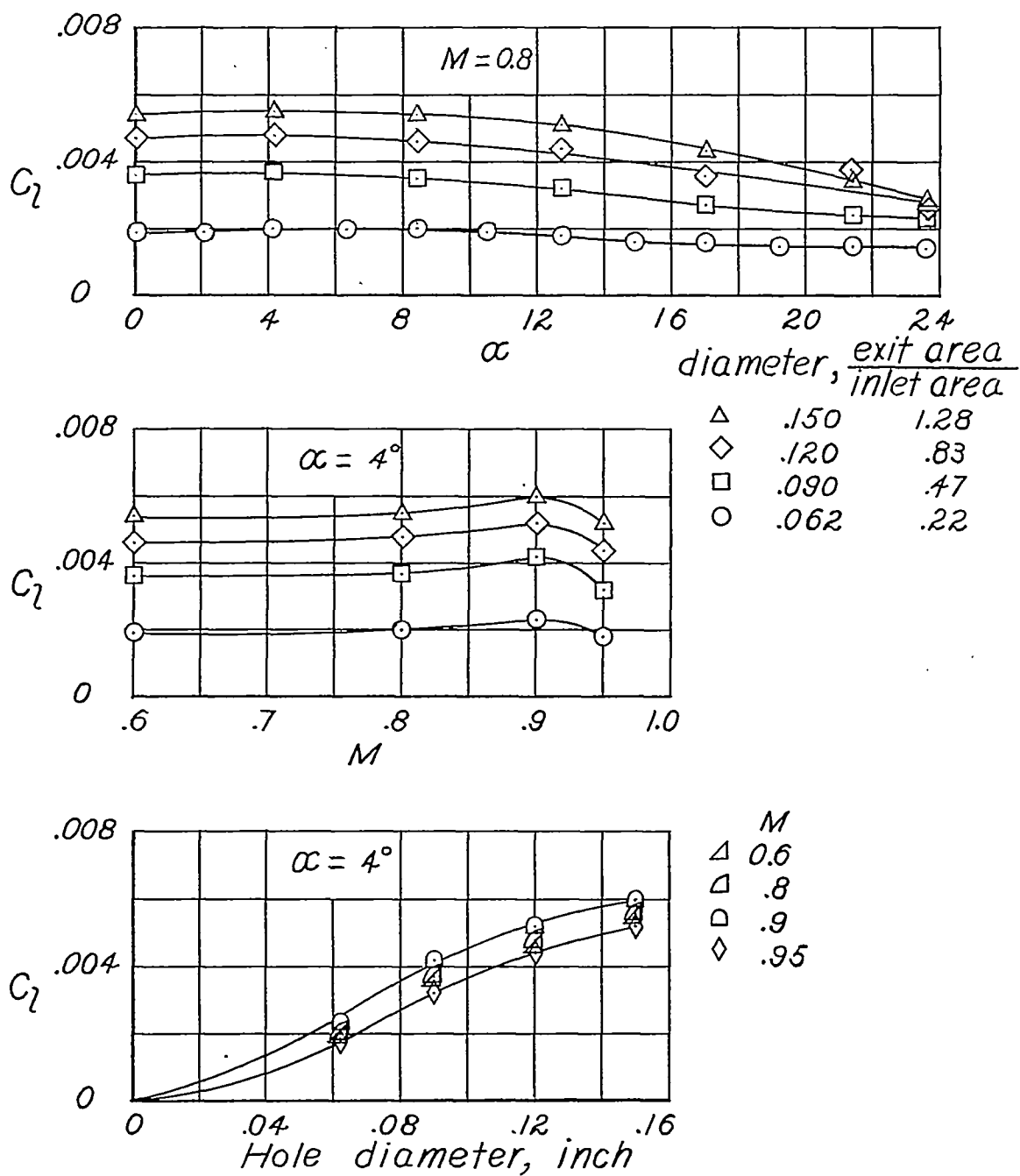
Figure 10.- Effect of jet hole size on the rolling-moment coefficients
of model 2(A) equipped with a jet control.
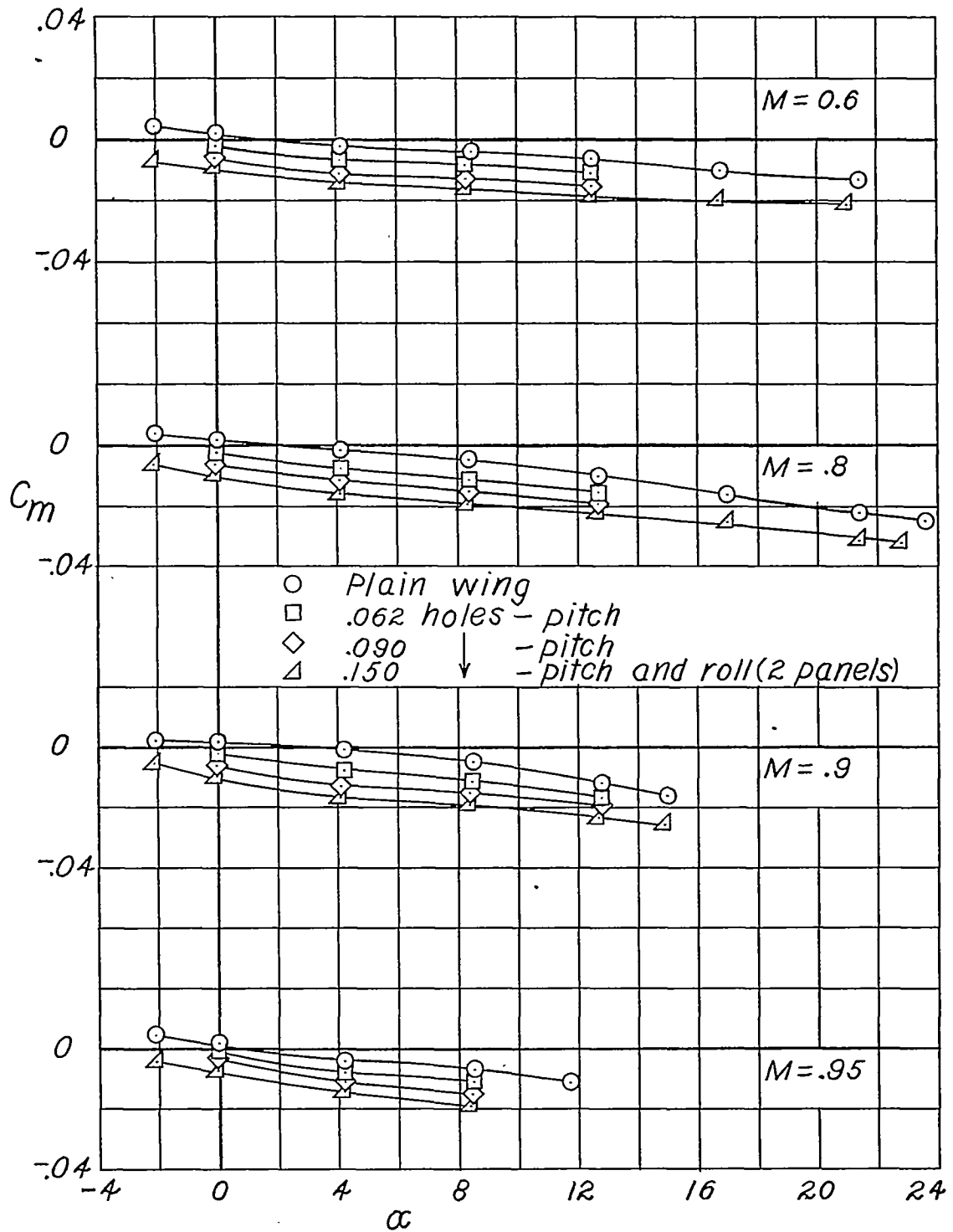
Figure 11.- Variation of pitching-moment coefficients with angle of attack of the plain-wing model 2(A) and the model with pitch controls of various size jet holes.
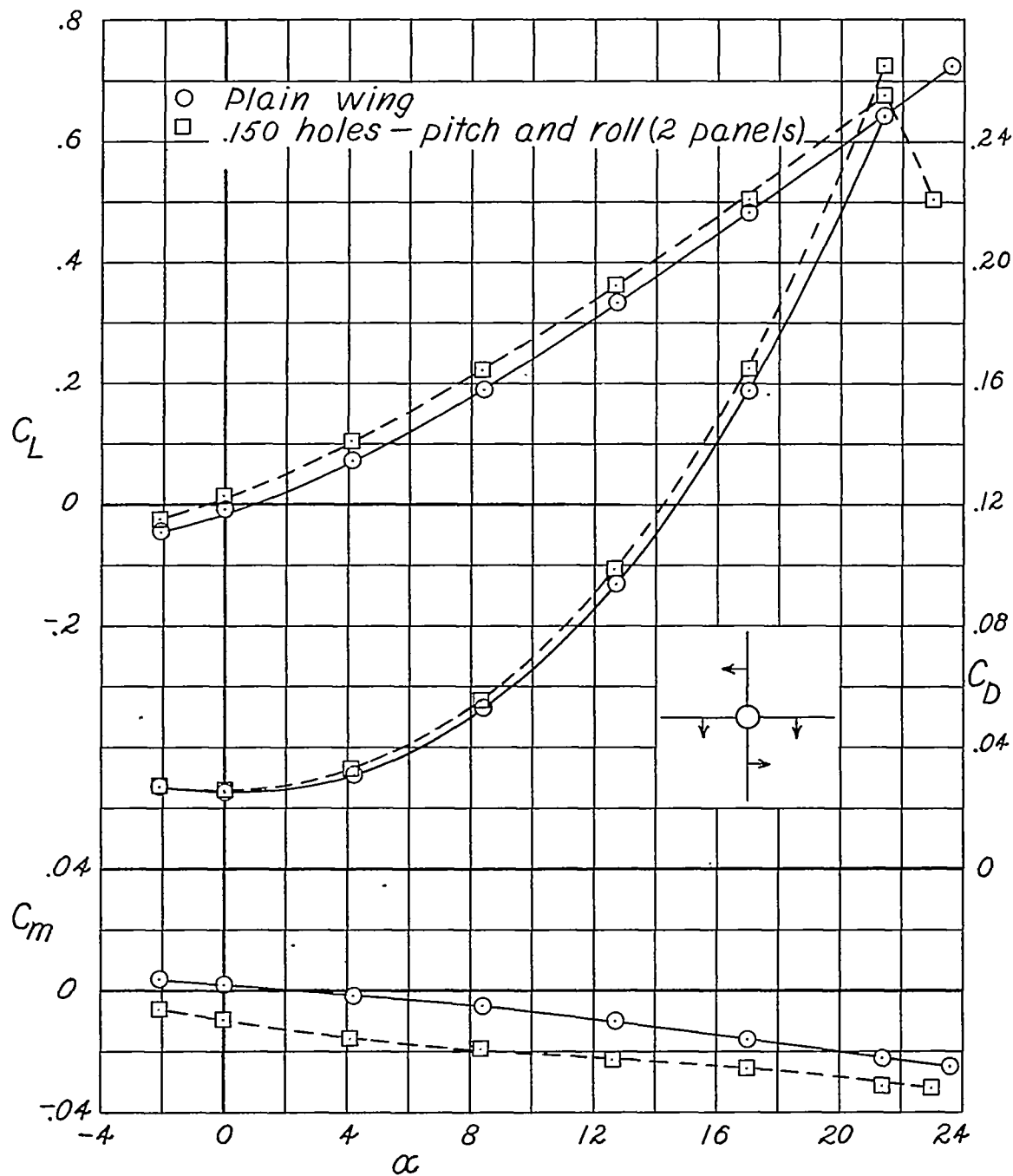
Figure 12.- Aerodynamic characteristics in pitch of the plain-wing (jet
holes sealed) model 2(A) and the model with pitch and roll controls.
M = 0.8.
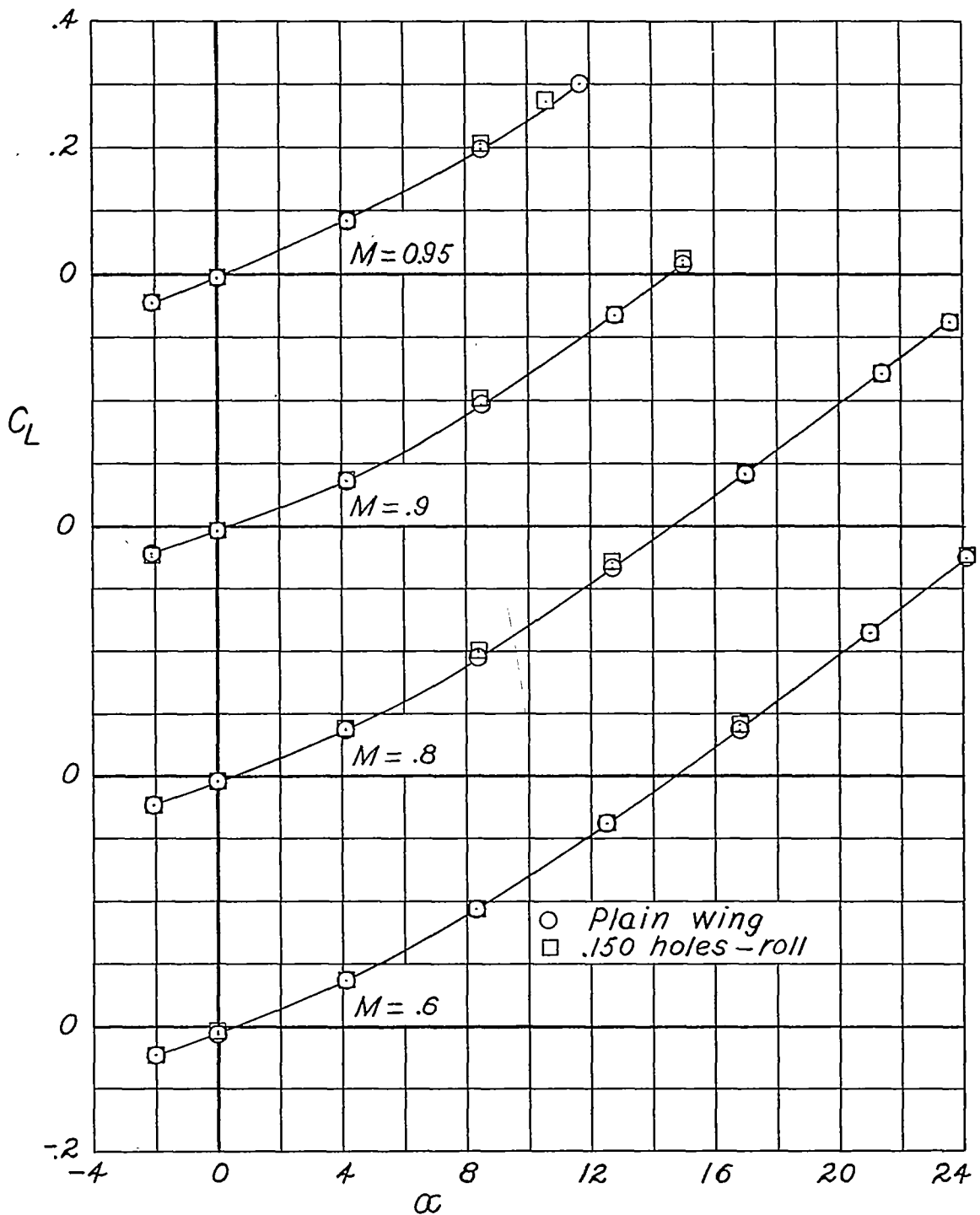
Figure 13.- Variation of lift coefficient with angle of attack of the
plain-wing model 2(A) and the model equipped with jet controls with
0.150-inch jet holes.
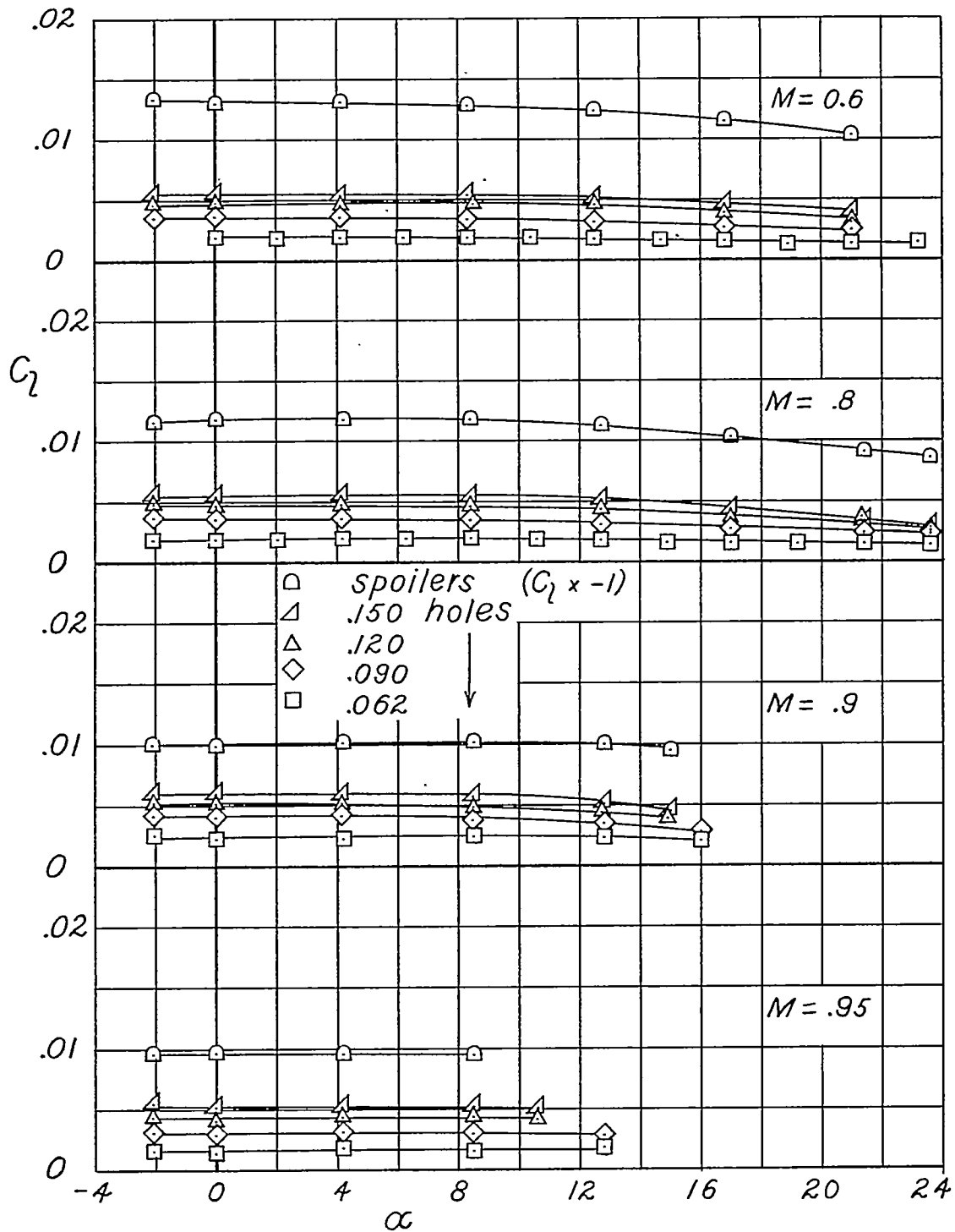
Figure 14.- Comparison of the rolling-moment coefficients resulting from jet controls (model 2(A)) and spoilers of 0.5-inch projection (model 2(B)).
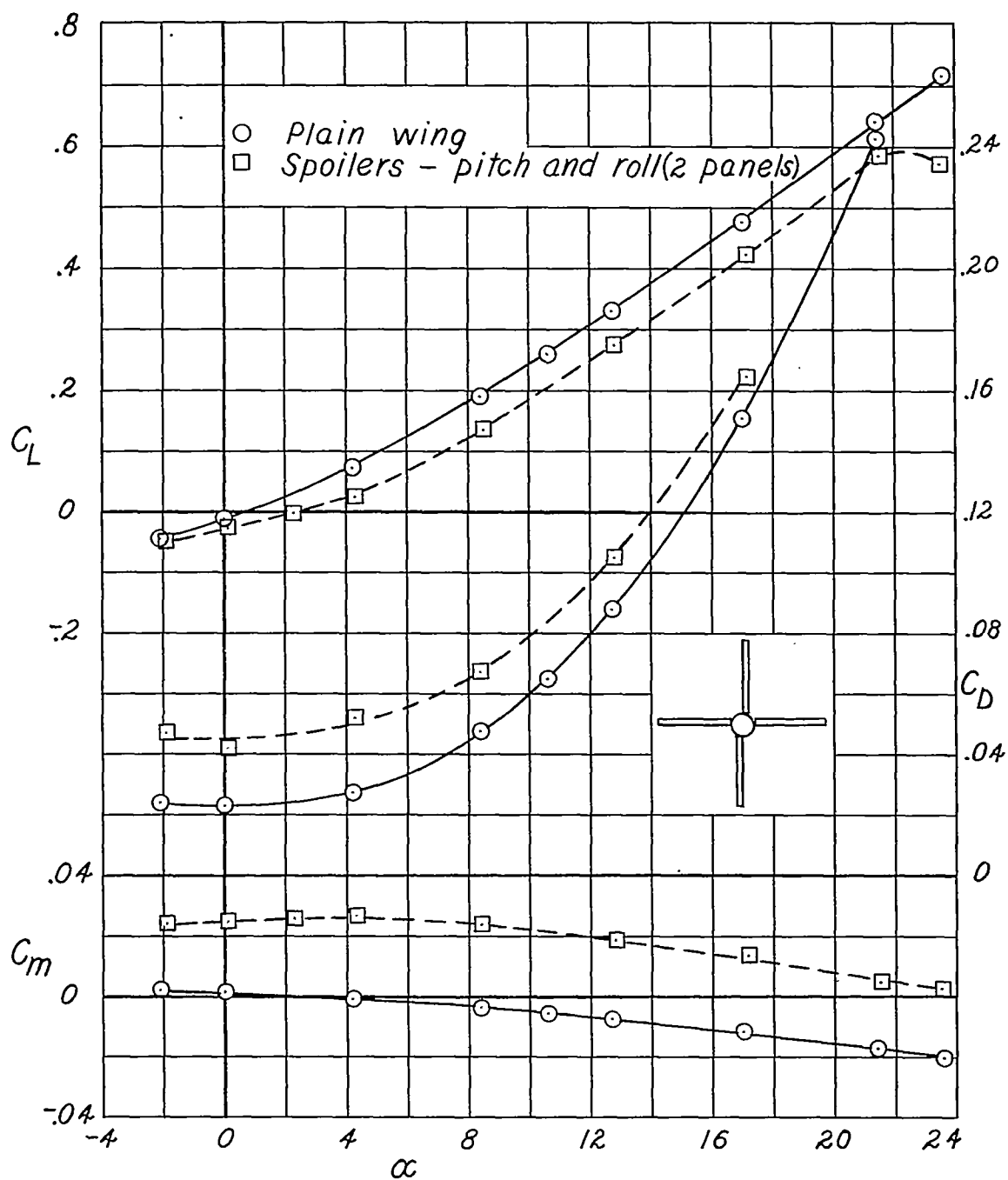
Figure 15.- Aerodynamic characteristics in pitch of model 2(B) with and without 0.5-inch spoilers producing pitch and roll.   M = 0.8.
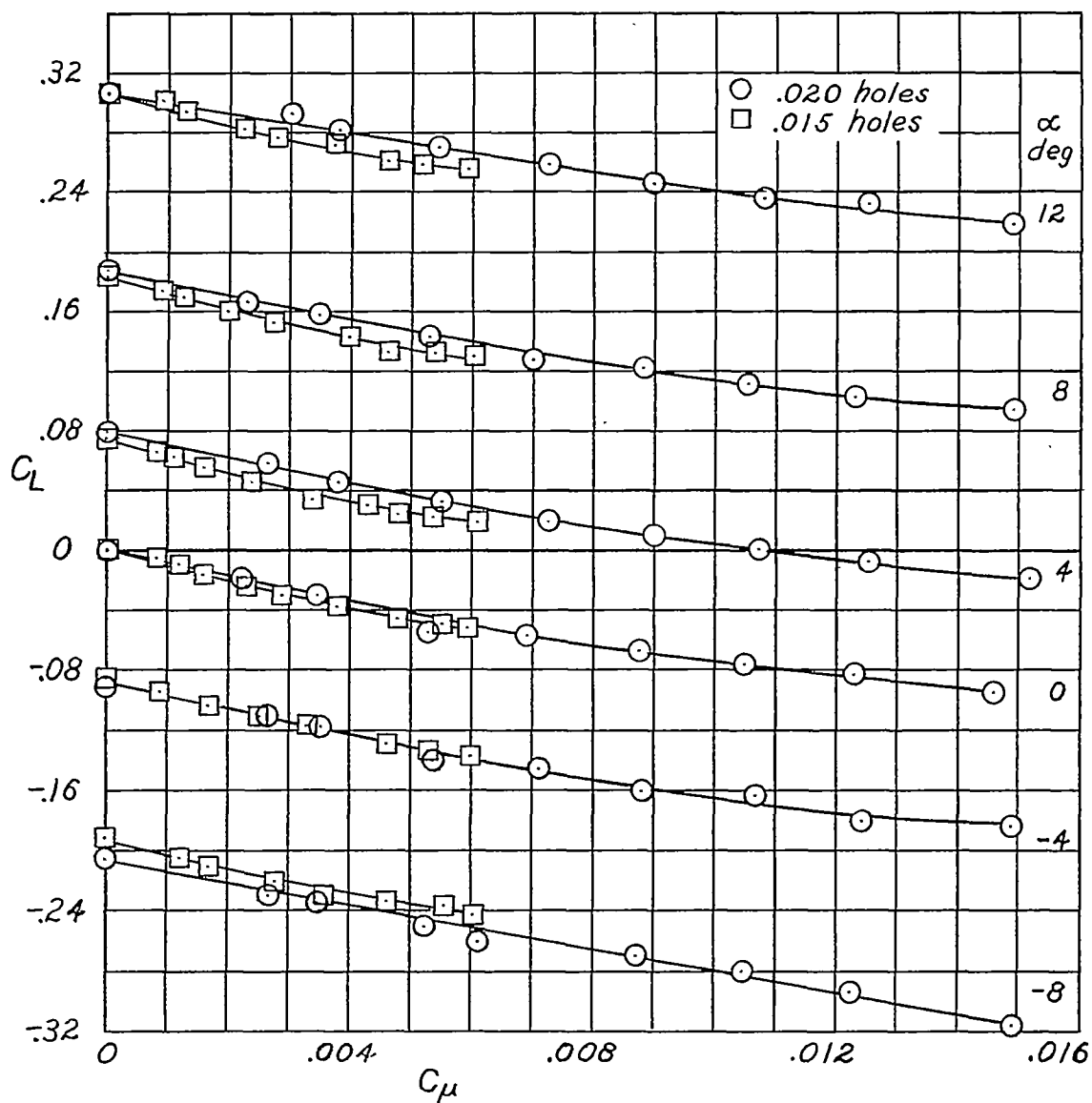
(a) M = 0.9.

Figure 16.- Variation of lift coefficient with momentum coefficient for
model 3 equipped with jet controls of two jet hole sizes.
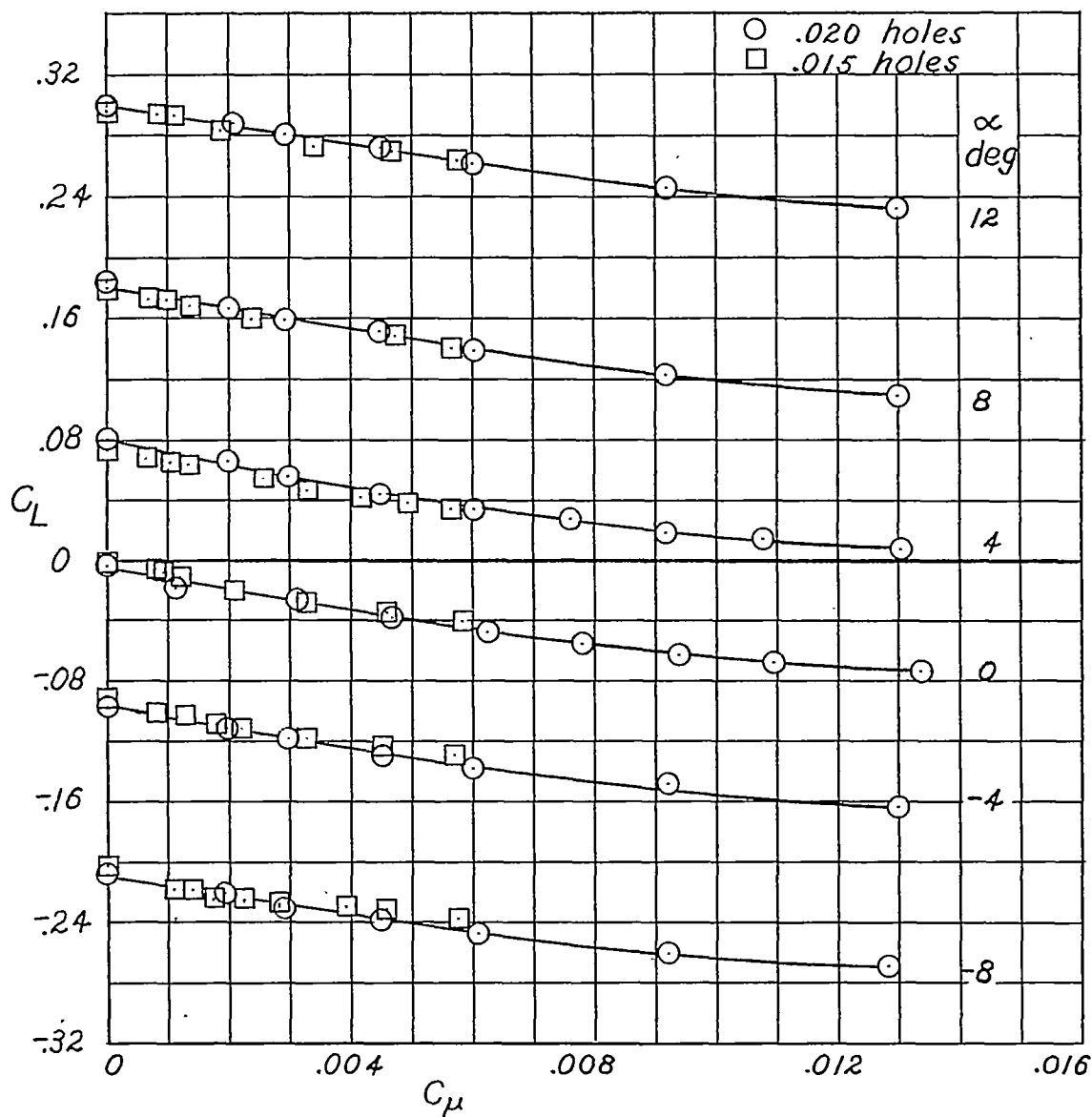
(b) M = 1.15.
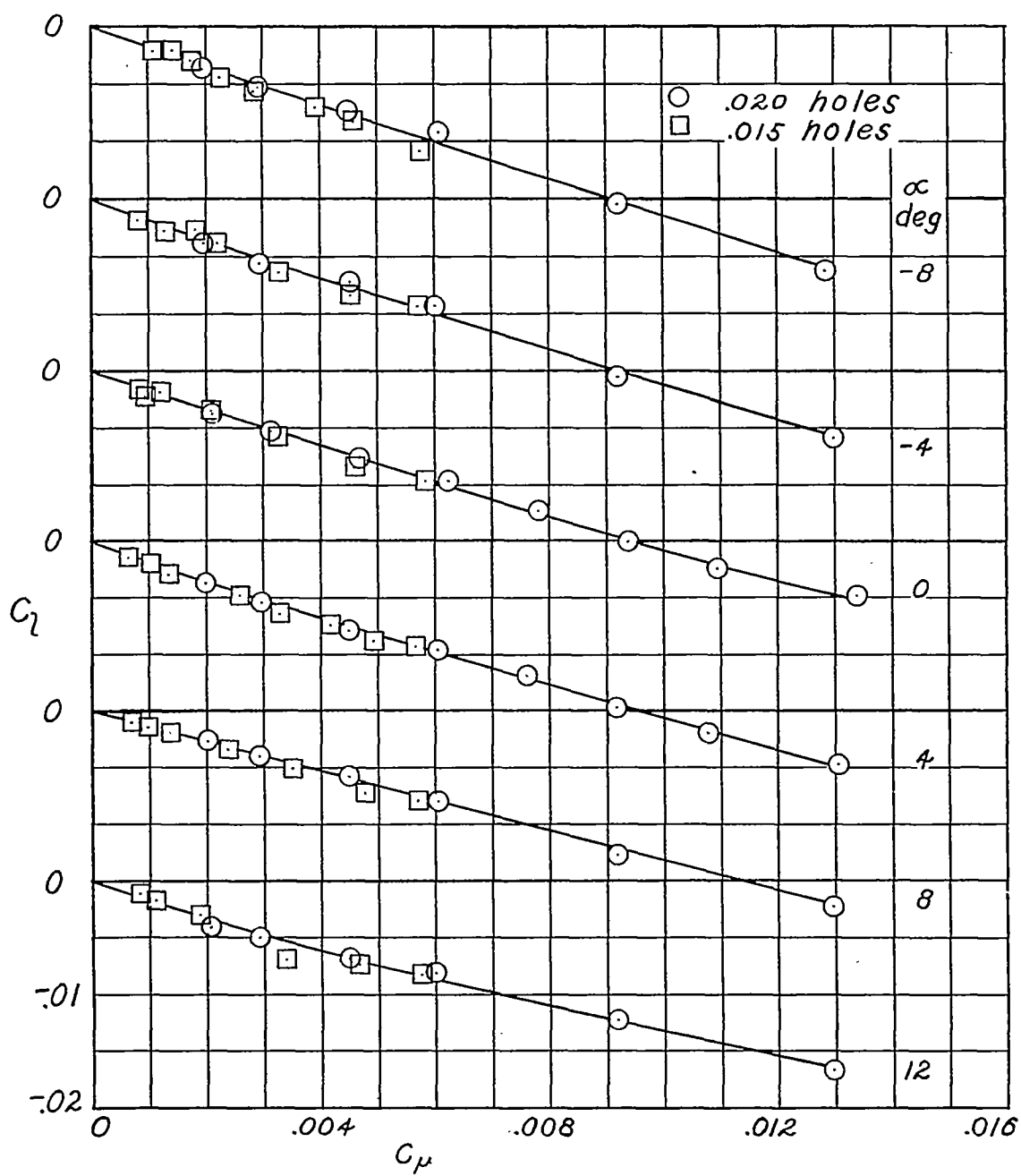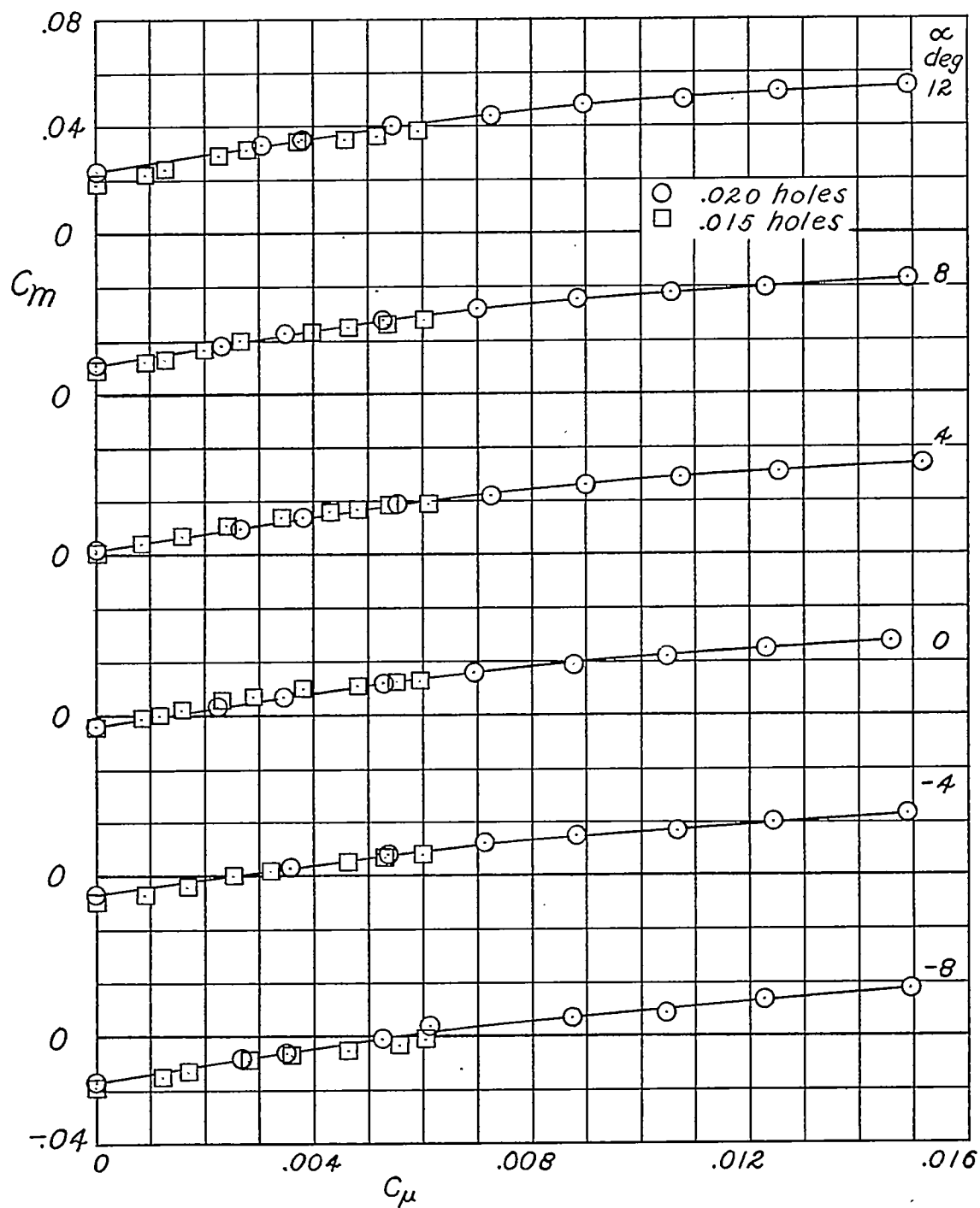
Figure 16.- Concluded.
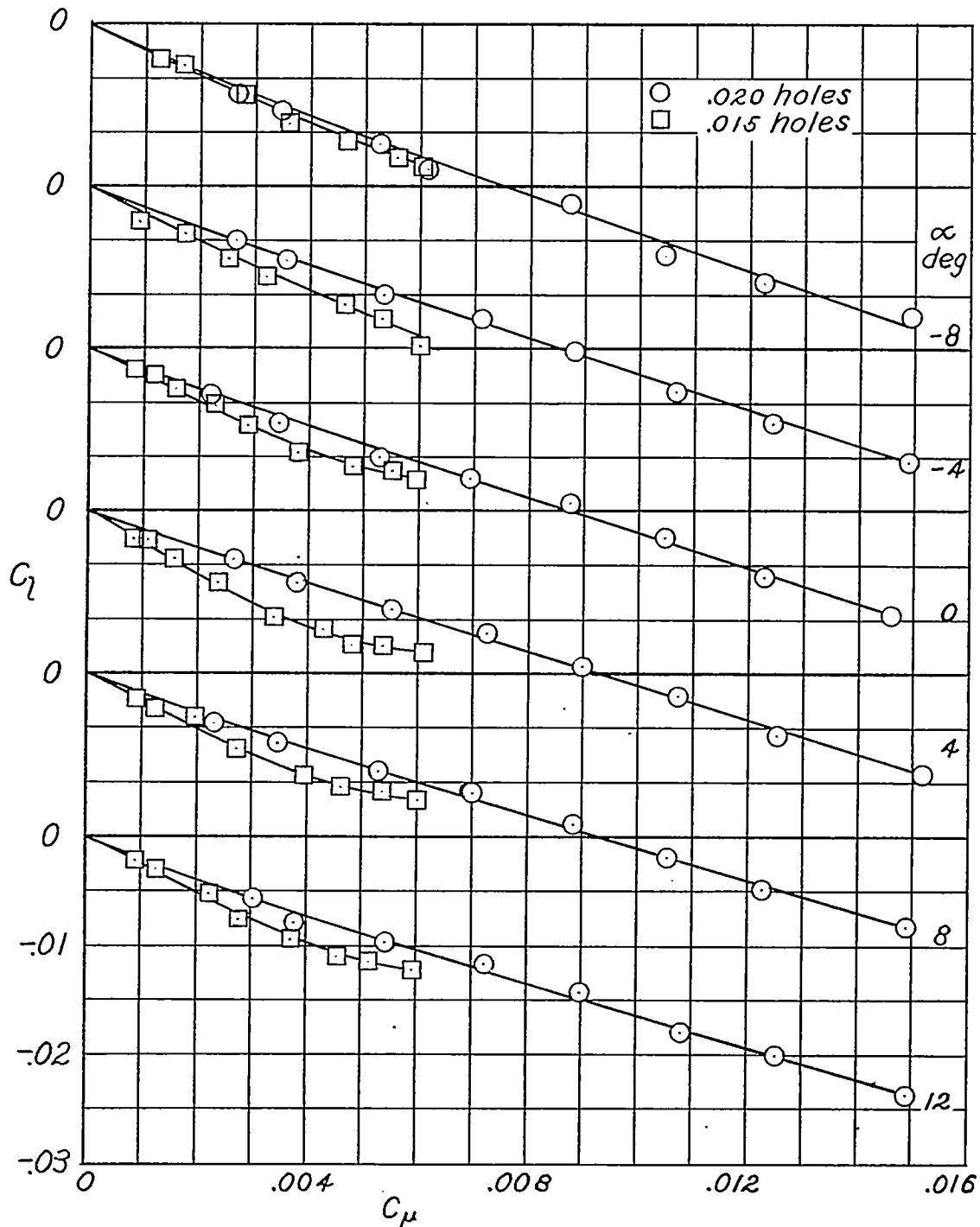
(a) M = 0.9.

Figure 17.- Variation of rolling-moment coefficient with momentum coeffi-
cient for model 3 equipped with jet controls of two jet hole sizes.
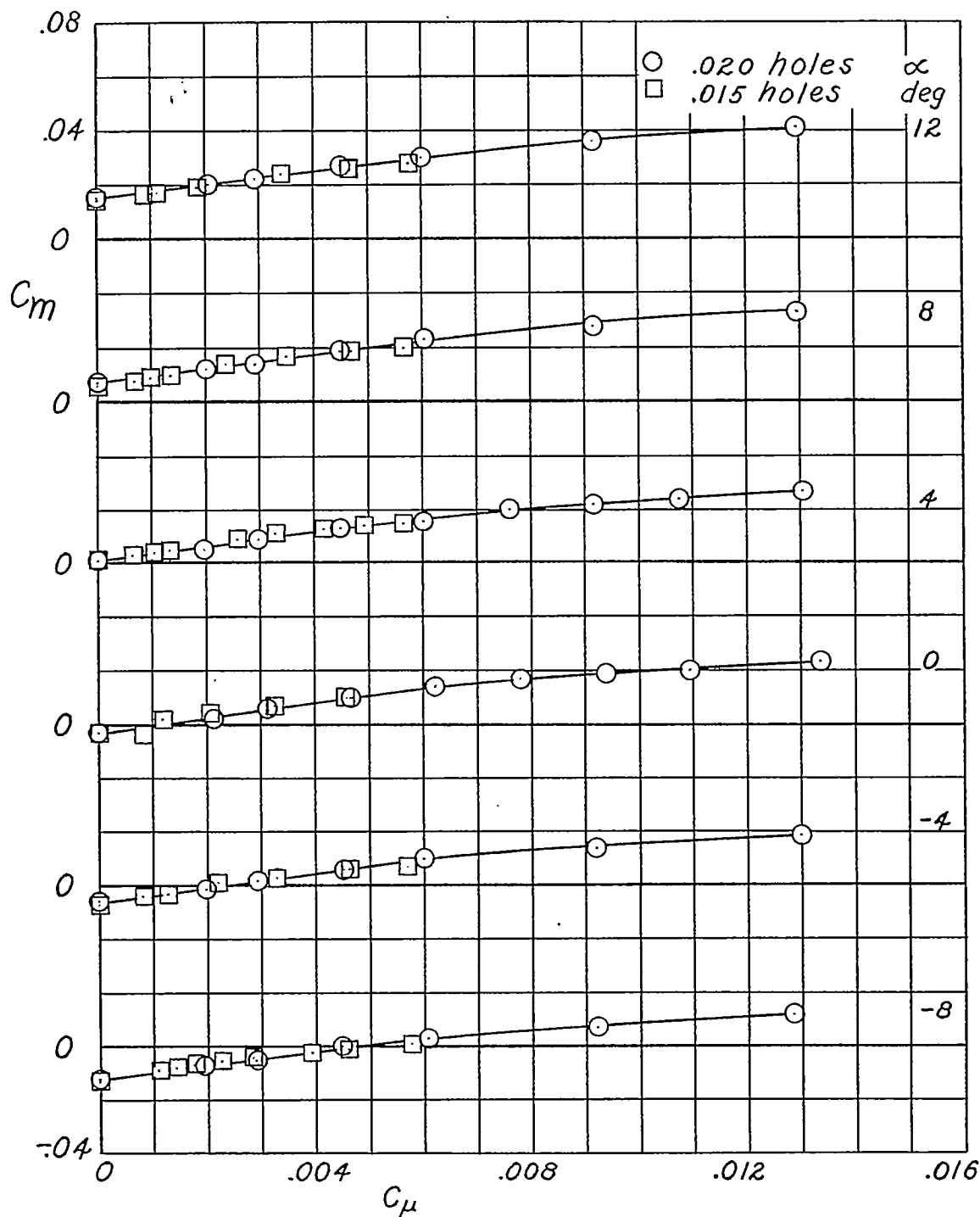
(b) M = 1.15.

Figure 17.- Concluded.

(a)   M = 0.9.

Figure 18.- Variation of pitching-moment coefficient with momentum coefficient for model 3 equipped with jet pitch controls of two jet hole sizes.

(b) M = 1.15.

Figure 18.- Concluded.
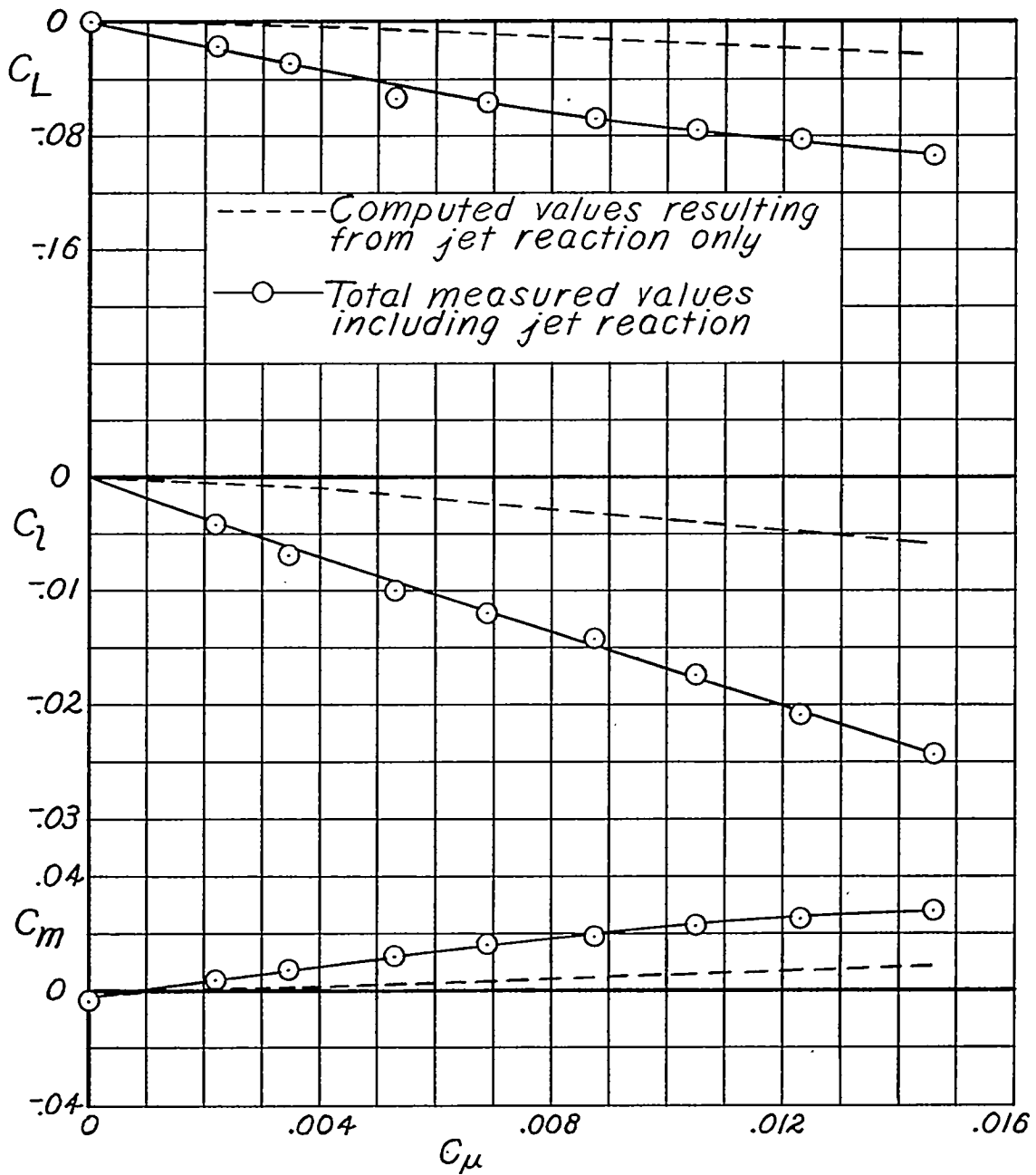
Figure 19.- Comparison of the total force and moment coefficients with those produced by the jet reaction only. $\alpha = 0°$; M = 0.9; 0.020-inch-diameter jets.